PROCEEDINGS OF SCIENCE

Global CKM Fits of the CKM Matrix with the Scan Method

Gerald Eigen,[*†]
University of Bergen
E-mail: gerald.eigen@ift.uib.no

Gregory Dubois-Felsmann, David G. Hitlin, Frank C. Porter
Caltech
E-mail: gpdf@slac.stanford.edu, hitlin@caltech.edu, fcp@caltech.edu

We present updated global fits of the CKM matrix with the Scan Method, now including the measurements of $B^0_s \to \mu^+\mu^-$ and $B^0_d \to \mu^+\mu^-$ branching fractions in the baseline fit. We explore the theory parameter space by scanning over three of the ten observables that have significant theory uncertainties. Furthermore, we explore the impact of a model that assumes new physics in $B^0_d \bar{B}^0_d$ mixing.

Flavor Physics & CP Violation 2015
May 25-29, 2015
Nagoya, Japan

[*]Speaker.
[†]This work is supported by the Norwegian research Council.

PoS(FPCP2015)083

1. Introduction and Fit Methodology

The phase of the Cabibbo-Kobayashi-Maskawa (CKM) matrix [1] produces *CP* violation in the Standard Model (SM). Unitarity relations of the CKM matrix provide an excellent laboratory to test the SM predictions, in particular the relation $V_{ub}^* V_{ud} + V_{cb}^* V_{cd} + V_{tb}^* V_{td} = 0$ since many measurements in the B and K systems can be combined for this test.

The scan method is a frequentist-based technique for fitting elements of the CKM matrix [2], making no assumptions as to the distribution of theory errors. We account for theory uncertainties in the QCD parameters $f_{B_s}, f_{B_s}/f_{B_d}, B_{B_s}, B_{B_s}/B_{B_d}$, and B_K and in the CKM parameters $|V_{ub}|$ and $|V_{cb}|$ by scanning over a plausible range of theory uncertainty using fixed grid or Monte Carlo (MC) methods. In the baseline fit, we combine measurements of $\Delta m_d, \Delta m_s, \varepsilon_K, |V_{cb}|, |V_{ub}|, |V_{ud}|, |V_{us}|$, $\sin 2\beta$, α, γ, $\mathscr{B}(B^+ \to \tau^+ \nu_\tau)$, $\mathscr{B}(B_s^0 \to \mu^+\mu^-)$ and $\mathscr{B}(B_s^0 \to \mu^+\mu^-)$ in the χ^2 function:

$$\begin{aligned}\chi^2(\bar\rho,\bar\eta,p_i,t_j) = & \left(\frac{\langle \Delta m_{d,s}\rangle - \Delta m_{d,s}(\bar\rho,\bar\eta,p_i,t_j)}{\sigma_{\Delta m_{d,s}}}\right)^2 + \left(\frac{\langle |V_{cb,ub,ud,us}|\rangle - V_{cb,ub,ud,us}(\bar\rho,\bar\eta,p_i,t_j)}{\sigma_{V_{cb,ub,ud,us}}}\right)^2 \\ & + \left(\frac{\langle |\varepsilon_K|\rangle - \varepsilon_K(\bar\rho,\bar\eta,p_i,t_j)}{\sigma_{\varepsilon_K}}\right)^2 + \left(\frac{\langle S_{\psi K^0}\rangle - \sin 2\beta(\bar\rho,\bar\eta,p_i)}{\sigma_{S_{\psi K^0}}}\right)^2 + \left(\frac{\langle \alpha\rangle - \alpha(\bar\rho,\bar\eta,p_i)}{\sigma_\alpha}\right)^2 \\ & + \left(\frac{\langle \gamma\rangle - \gamma(\bar\rho,\bar\eta,p_i)}{\sigma_\gamma}\right)^2 + \sum_k \left(\frac{\langle \mathscr{M}_k\rangle - \mathscr{M}_k(p_i)}{\sigma_{\mathscr{M}_k}}\right)^2 + \sum_n \left(\frac{\langle \mathscr{T}_n\rangle - \mathscr{T}_n(p_i,t_j)}{\sigma_{\mathscr{T}_n}}\right)^2, \end{aligned} \tag{1.1}$$

where p_i are measured quantities, including the Wolfenstein parameters A and λ; the t_j are QCD parameters. Errors on the t_j are split into a "statistical" and a theory error. We account for the "statistical" error by including terms in the χ^2 denoted by $\mathscr{T}_n$ in which the central values are taken from lattice calculations; we perform scans over the theory errors. To account for correlations among the observables, we add χ^2 terms, denoted by $\mathscr{M}_k$, that include branching fractions, other CKM elements, Higgs, quark and B meson masses, and B meson lifetimes. Table 1 lists measured input values for baseline fits. Table 2 summarizes all the QCD parameters including $\eta_{cc}, \eta_{tc}, \eta_{tt}$ and η_b. We presently do not scan over the latter parameters, but account for them in the $\mathscr{T}_n$ terms. We parametrize η_{cc} and its uncertainty in terms of m_c and α_s. For each choice of a set of theory parameters, we determine the χ^2 and $P(\chi^2 \geq \chi^2_c; n-p+2|H_0) \geq 0.05$ where $n(p)$ are the number of χ^2 terms (number of fit parameters) and H_0 is the test hypothesis (*e.g.* the SM). For fits with $P(\chi^2) > 5\%$, we plot $\bar\rho - \bar\eta$ contours. The overlay of all contours present the $\bar\rho - \bar\eta$ region allowed in the SM. From the extrema of all displayed contours, we determine the range of UT parameters for a given confidence interval having made no assumption as to the distribution of theory errors.

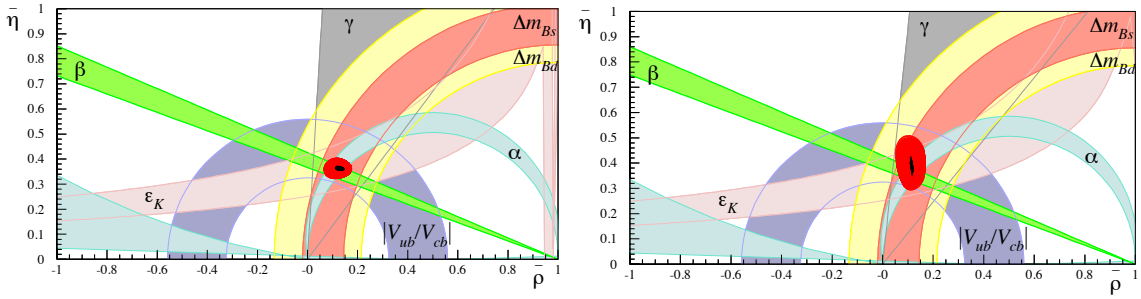

Figure 1: Overlay of 95% CL contours in the $\bar\rho - \bar\eta$ plane for the baseline fits without (left) and with NP parameters r_d and θ_d (right).

Table 1: Observables used in the baseline fits [3, 4].

m_t [GeV/c^2]	m_c [GeV/c^2]	Δm_d [ps^{-1}]	Δm_s [ps^{-1}]
173.2 ± 0.87	1.275 ± 0.025	0.510 ± 0.003	17.757 ± 0.021
$\lvert V_{cb}\rvert$	$\lvert V_{ub}\rvert$	$\lvert V_{ud}\rvert$	$\lvert V_{us}\rvert$
$(4.09 \pm 0.06 \pm 0.11) \times 10^{-2}$	$(4.15 \pm 0.1 \pm 0.48) \times 10^{-3}$	0.97425 ± 0.00022	0.2252 ± 0.0009
$\lvert V_{cd}\rvert$	$\lvert V_{cs}\rvert$	$\lvert V_{tb}\rvert$	
0.23 ± 0.11	1.006 ± 0.023	0.97 ± 0.08	
ε_K	$\sin 2\beta$	α	γ
$(2.228 \pm 0.0011) \times 10^{-3}$	0.0691 ± 0.017	$(85.1^{+2.2}_{-2.0})^o$	$(68.5^{+7.9}_{-9.0})^o$
$\mathscr{B}(B^+ \to \tau^+\nu)$	$\mathscr{B}(B_s^0 \to \mu^+\mu^-)$	$\mathscr{B}(B_d^0 \to \mu^+\mu^-)$	
$(1.14 \pm 0.27) \times 10^{-4}$	$(2.8^{+0.7}_{-0.6}) \times 10^{-9}$	$(3.9^{+1.6}_{-1.4}) \times 10^{-10}$	

Table 2: QCD parameters used in the fits with "statistical" and theory uncertainties, respectively [5].

f_{B_s} [MeV]	f_{B_s}/f_{B_d}	B_{B_s}	B_{B_s}/B_{B_d}	B_K
$228.7 \pm 2.0 \pm 5.5$	$1.311 \pm 0.046 \pm 0.076$	$1.205 \pm 0.009 \pm 0.019$	$1.053 \pm 0.04 \pm 0.064$	$0.758 \pm 0.0020 \pm 0.019$
η_{cc}	η_{tc}	η_{tt}	η_b	
1.39 ± 0.35	0.47 ± 0.04	0.5765 ± 0.0065	0.551 ± 0.007	

Table 3: The 95% CL ranges from baseline fits without/with $\mathscr{B}(B_{s,d} \to \mu^+\mu^-)$ for UT parameters.

Parameter	$\bar{\rho}$	$\bar{\eta}$	β [^{o}]	α [^{o}]	γ [^{o}]
Baseline fit without $B_{s,d} \to \mu^+\mu^-$	$0.077 - 0.176$	$0.322 - 0.400$	$19.9 - 24.9$	$80.2 - 93.8$	$63.6 - 77.8$
Baseline fit with $B_{s,d} \to \mu^+\mu^-$	$0.069 - 0.172$	$0.324 - 0.401$	$19.8 - 24.8$	$79.0 - 93.3$	$64.2 - 79.2$
New physics fit with $B_{s,d} \to \mu^+\mu^-$	$0.052 - 0.168$	$0.294 - 0.509$	$18.2 - 29.9$	$70.0 - 95.1$	$64.2 - 83.4$

2. Results

Figure 1 (left) shows the overlay of $\bar{\rho} - \bar{\eta}$ contours for all accepted baseline fits using 24 measurements ($|V_{ud}|$, $|V_{us}|$, $|V_{cb}|$, $|V_{cb}|$, $|V_{cd}|$, $|V_{cs}|$, $|V_{tb}|$, ε_K, Δm_{B_d}, Δm_{B_s}, $\sin 2\beta$, α, γ, f_{B_s}, B_{B_s}, $f_{B_s/f_{B_d}}$, B_{B_s}/B_{B_d}, B_K, m_t, m_c, $\mathscr{B}(B^+ \to \tau^+\nu)$, $\mathscr{B}(B_s^0 \to \mu^+\mu^-)$ and $\mathscr{B}(B_d^0 \to \mu^+\mu^-)$) to fit 12 parameters ($\bar{\rho}$, $\bar{\eta}$, A, λ, f_{B_s}, B_{B_s}, $f_{B_s/f_{B_d}}$, B_{B_s}/B_{B_d}, B_K, m_t, m_c and M_H). Table 3 shows the 95% CL range of the unitarity triangle (UT) parameters for baseline fits without and with $\mathscr{B}(B_{s,d}^0 \to \mu^+\mu^-)$.

New physics in $B_d^0\bar{B}_d^0$ mixing can be parameterized by a scale factor r_d and a phase ϕ_d since

$$\langle \bar{B}_d^0 | \mathscr{H}^{NP} + \mathscr{H}^{SM} | B^0 \rangle / \langle \bar{B}_d^0 | \mathscr{H}^{SM} | B^0 \rangle \equiv r_d^2 \exp(2i\theta_d) \tag{2.1}$$

where $\mathscr{H}^{NP}(\mathscr{H}^{SM})$ represent the new physics (SM) Hamiltonian. The scale factor modifies Δm_{B_d} to $(\Delta m_{B_d})^{NP} = r_d^2 (\Delta m_{B_d})^{SM}$ and $(\Delta m_{B_s}/\Delta m_{B_d})^{NP} = (1/r_d^2)(\Delta m_{B_s}/\Delta m_{B_d})^{SM}$, and the phase modifies observables containing $\sin 2\beta$ and $\sin 2\alpha$ to $\sin 2(\beta + \theta_d)$ and $\sin 2(\alpha - \theta_d)$. To test this model, we add r_d and θ_d to the baseline fit. Figure 1 (right) shows the resulting $\bar{\rho} - \bar{\eta}$ contours for all accepted baseline fits. The allowed region increases since the Δm_{B_d}, $\Delta m_{B_s}/\Delta m_{B_d}$, $\sin 2\beta$ and $\sin 2\alpha$ constraints are weakened due to compensation by the parameters r_d and θ_d. Figure 2 shows the $r_d - \theta_d$ contours that are consistent with the SM prediction.

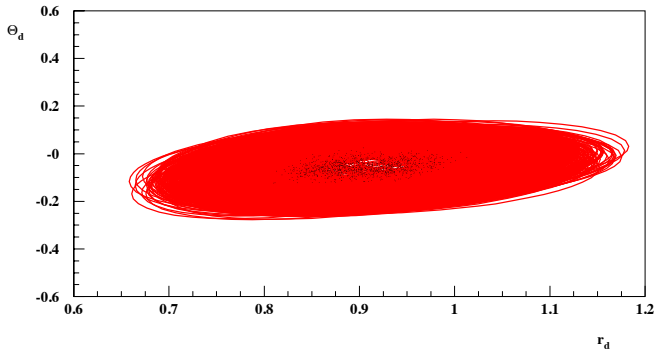

Figure 2: Overlay of $r_d - \theta_d$ contours. Black points show central values; the SM prediction is at (1,0).

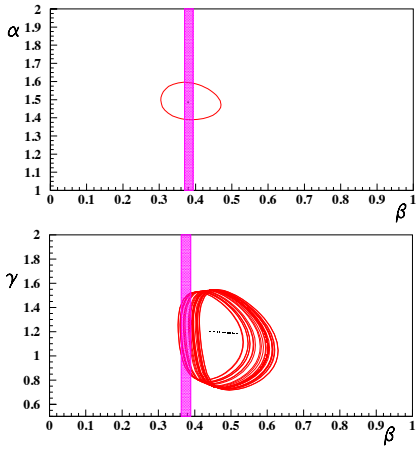

Figure 3: The $\alpha - \beta$ (top) and $\gamma - \beta$ contours (bottom). Black points show central values; the magenta band shows the world average on β measured in $(c\bar{c})K^{(*)}$ modes.

We further perform fits, called full fits, in which we replace α and γ by measurements that determine them. These consist of all branching fractions and *CP* asymmetries measured in $B \to PP$, PV, VV modes and measurements of decay ratios and *CP* asymmetries of $B^+ \to D^{(*)}K^+$ and $B^+ \to DK^{*+}$, $B^+ \to D^{(*)}\pi^+$ and $B^0 \to D^{(*)+}\rho^-$ decays analyzed in the Giri-Grossman-Soffer-Zupan [6], Gronau-London-Wyler [7] and Atwood-Dunietz-Soni (ADS) methods [8]. Omitting $\mathscr{B}(B^+ \to \tau^+\nu)$ and $\mathscr{B}(B_{s,d} \to \mu^+\mu^-)$, we fit to 230 measurements to determine 104 parameters. Following the Gronau-Rosner approach [9], we parametrize amplitudes in terms of tree, color-suppressed tree, penguin, singlet penguin, W-annihilation/W-exchange and electroweak-penguin diagrams (up to λ^2 beyond leading order). In full fits, possible correlations between $\alpha(\gamma)$ and β are accounted for, which is typically not the case in our baseline fits and fits by CKMfitter [10] and UTFIT [11].

We use the methodology of full fits to determine α and γ. We fit to 184 branching fractions and *CP* asymmetry measurements in $B \to PP$, $B \to PV$, $B \to VV$ and $B \to a_1 P$ modes to determine 95 parameters and extract $\alpha - \beta$ contours at 95% CL shown in Fig. 3 (top). We fit to 61 rate ratio and *CP* asymmetry measurements in $B^\pm \to D^{(*)0}K^\pm$, $B^\pm \to D^0 K^{*\pm}$, $B^\pm \to D^{(*)0}\pi^\pm$ and $B^\pm \to D^0\rho^\pm$ modes to determine 20 parameters and extract $\gamma - \beta$ contours at 95% CL shown in Fig. 3 (bottom) after scanning over $|V_{ub}/V_{cb}|$. Table 4 shows the fit results. Both $\alpha - \beta$ and $\gamma - \beta$ contours are consistent with the world average of $\beta = (21.9 \pm 0.7)^\circ$ from $B \to (c\bar{c})K^{(*)}$ measurements [4]. Note that α and γ are correlated with β and that γ depends on $|V_{ub}/V_{cb}|$.

Table 4: Measurements of α from fits to branching fractions and *CP* asymmetries in $B \to PP, PV, VV, a_1 P$ decays and measurements of γ from fits to rate ratios and *CP* asymmetries in $B^\pm \to D^{(*)0}K^\pm$, $B^\pm \to D^0 K^{*\pm}$, $B^\pm \to D^{(*)0}\pi^\pm$ and $B^\pm \to D^0\rho^\pm$ modes. The different γ values result from the lowest/highest values of $|V_{ub}/V_{cb}|$. The magenta bar shows the world average for β from $B \to c\bar{c}K^{(*)}$ modes.

Mode	α [^{o}]	β [^{o}]	γ [^{o}]
$B \to PP, PV,$ $VV, a_1 P$	$85.2^{+2.1}_{-2.0}$	$21.7^{+1.7}_{-1.6}$	
$B \to D^{(*)}h$		$30.5^{+2.3}_{-2.2}$ $24.8^{+2.0}_{-2.0}$	$67.7^{+7.9}_{-9.2}$ $69.1^{+7.8}_{-8.8}$

3. "Wall" Plots

We construct "Wall" plots to display the correlations among sets of three parameters. Orthogonal lines show the $\pm 1\delta$ theory error range. The outer black contours result from probability

requirements of $> 32\%$ or $> 5\%$. The inner black contours result from a $\pm 1\delta$ requirement on all undisplayed variables. Colored solid contours result from a $\pm 1\delta$ requirement on the out-of-plane variables. Colored dashed contours result from constraining the out-of-plane variables to their central values. Black dashed contours result from constraining all undisplayed variables to their central values. Figure 4 shows "Wall" plots for $|V_{ub}|$, f_{B_s} and B_{B_S} for $P(\chi^2) > 32\%$ and $P(\chi^2) > 5\%$.

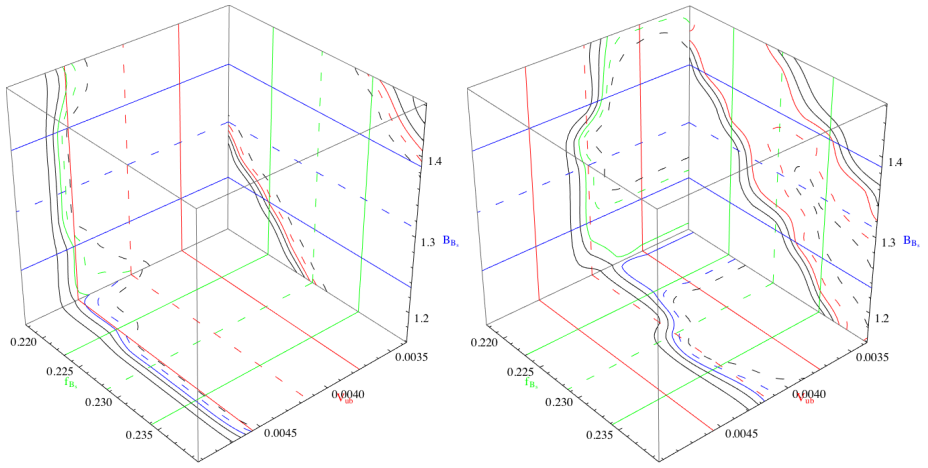

Figure 4: Wall plots for $|V_{ub}|$, f_{B_s} and B_{B_S} for $P(\chi^2) > 5\%$ (left) and $P(\chi^2) > 32\%$ (right).

4. Conclusion

Scan method baseline fits and full fits agree with the SM with no assumption as to the distribution of theory errors. The latter include correlations among α (γ) and β. Dedicated fits to α and γ yield rather precise values. A new physics model in $B^0_d\bar{B}^0_d$ mixing increases the allowed $\bar{\rho} - \bar{\eta}$ region. "Wall" plots provide a means to determine whether any SM discrepancy originates from the values of theory parameters, experimental measurements or something else.

References

[1] N. Cabibbo, PRL **10**, 531 (1963); M. Kobayashi, T. Maskawa, Prog.Th.Phys. **49**, 652 (1973).

[2] G. Eigen *et al.*, PRD **89** 033004 (2014).

[3] J. Beringer *et al.* (Particle Data Group), PR **D86**, 010001 (2012).

[4] D. Asner *et al.*, arXiv:1010.1589v3 (2011); www.slac.stanford.edu/xorg/hfag/triangle/index.html

[5] J. Laiho *et al.*, http://mypage.iu.edu/ elunghi/webpage/LatAves.

[6] A. Giri *et al.*, PR **D68**, 054018 (2003).

[7] M. Gronau, D. London, PL**B 253**, 483 (1991); M. Gronau, D.Wyler, PL**B 265**, 172 (1991).

[8] D. Atwood, I. Dunietz, A. Soni, PRL **78**, 3257 (1997); PR**D 63**, 036005 (2001).

[9] M. Gronau *et al.*, PR**D 50**, 4520 (1994); PR**D 60**, 034021 (1999); PR**D 61**, 073008 (2000); PR**D 62**, 014031 (2000); PR**D 69**, 119901 (2004); A.S. Dighe *et al.*, PR**D 57**, 1783 (1998); A. Beneke *et al.*, PL**B 638**, 68 (2006).

[10] J. Charles *et al.*, Eur. Phys. Jour. **C41**, 1 (2005); updates at http://ckmfitter.in2p3.fr/.

[11] M. Bona *et al.*, JHEP **803**, 049 (2008); updates at http://www.utfit.org/.